Available online at www.sciencedirect.com
SCIENCE DIRECT
Biochemical and Biophysical Research Communications 341 (2006) 158–166
BBRC
www.elsevier.com/locate/ybbrc

A novel iron responsive element in the 3′UTR of human MRCKα ☆

Radek Cmejla *, Jiri Petrak, Jana Cmejlova

Institute of Hematology and Blood Transfusion, Department of Cell Physiology, U Nemocnice 1, Prague, 128 20, Czech Republic

Received 18 December 2005
Available online 6 January 2006

Abstract

Human untranslated region (UTR) databases were searched to identify novel proteins potentially regulated by an iron responsive element (IRE), and found two candidates—cell cycle phosphatase Cdc14A variant 1 and myotonic dystrophy kinase-related Cdc42-binding kinase α (MRCKα), both possessing a putative IRE in their 3′UTR. In further experiments, we focused on MRCKα. Biochemical analyses of the MRCKα IRE revealed that it was functional and mediated the response to iron level in the same way as transferrin receptor 1 IREs (TfR) did. Similar to *TfR* mRNA, *MRCKα* mRNA is stabilized, when iron supply is low, while it is destabilized under iron-rich conditions. The expression of *MRCKα* mRNA was found to be ubiquitous; the highest levels were noted in testes, the lowest in skeletal muscle. The level of *MRCKα* mRNA in various tissues strongly positively correlates with the level of *TfR* mRNA, indicating its possible role in the transferrin iron uptake pathway.

Keywords: Myotonic dystrophy kinase-related Cdc42-binding kinase α; MRCKα; CDC42BPA; Iron responsive element; IRE; Transferrin receptor 1

RNA-binding proteins play a key role in RNA posttranscriptional processing, such as splicing, nucleo-cytoplasmic transport, localization, translation, stability or degradation. It is therefore of great importance to identify RNA-binding proteins and their respective RNA recognition elements to understand basic cellular processes.

Binding of iron regulatory proteins (IRP1 and IRP2) to iron responsive elements (IREs) located in 3′ or 5′ untranslated regions (3′ or 5′UTR) of some mRNAs is among the best characterized RNA/protein interactions [1]. IREs are phylogenetically conserved in vertebrates and form hairpin structures consisting of ~30 nucleotides. The IRE loop sequence CAGU/AGH (H is A, U, and C) is well conserved; an upper stem of five perfectly paired bases is separated from a lower stem by a single cytosine (or two nucleotides and cytosine in ferritin) [2,3].

The list of IRE-regulated proteins in humans comprises H-ferritin, L-ferritin, the erythroid isoform of 5-aminolevulinate synthase, mitochondrial aconitase and ferroportin with an IRE in 5′UTR, and transferrin receptor 1 (TfR) and one isoform of divalent metal ion transporter 1 (DMT1, SLC11A2) with an IRE in 3′UTR [1,4]. In iron-depleted cells, IRPs bind to the IRE with high affinity, while in iron-replete cells they fail to bind IREs. It is believed that binding of IRPs to the 5′UTR IRE blocks translation, while binding to the 3′UTR IRE increases mRNA stability [2]. By these mechanisms, cellular processes dependent on the intracellular iron level (mainly iron metabolism) can be controlled.

Using a computer search in UTR databases we identified two human proteins with a putative IRE sequence in their 3′UTR—cell cycle phosphatase Cdc14A variant 1 and myotonic dystrophy kinase-related Cdc42-binding kinase α (MRCKα, official symbol CDC42BPA). Biochemical analyses of MRCKα IRE revealed that it was recognized by IRPs, and it mediated the response to iron levels in the same way as IREs in the transferrin receptor 1 did.

☆ *Abbreviations:* 2ME, 2-mercaptoethanol; ARE, AU-rich element; Desf, desferrioxamine; DMT1, divalent metal ion transporter 1; DRB, 5, 6-dichlorobenzimidazole riboside; EMSA, electrophoretic mobility-shift assay; GAPDH, glyceraldehyde-3-phosphate dehydrogenase; IRE, iron responsive element; IRP, iron regulatory protein; MRCKα, myotonic dystrophy kinase-related Cdc42-binding kinase α; Tf, diferric transferrin; TfR, transferrin receptor 1; UTR, untranslated region.

* Corresponding author. Fax: +420 221 977 370.
E-mail addresses: racm@centrum.cz, cmejla@uhkt.cz (R. Cmejla).

0006-291X/$ - see front matter © 2006 Elsevier Inc. All rights reserved.
doi:10.1016/j.bbrc.2005.12.155

MRCKα is the effector of a small Rho GTPase Cdc42 and together they promote cytoskeletal reorganization [5]. The identification of an IRE sequence in the *MRCKα* mRNA represents a novel molecular link between iron metabolism and the cellular cytoskeleton.

Materials and methods

Databases, bioinformatics. To search for putative IREs, the PatSearch program was used at bighost.area.ba.cnr.it/BIG/PatSearch. The pattern for an IRE was defined as r1 = {au,ua,gc,cg,gu,ug} (p1 = 2...8 c p2 = 5...5 cagwgh r1 ∼ p2 r1 ∼ p1 | p3 = 2...8 nnc p4 = 5...5 cagwgh r1 ∼ p4 n r1 ∼ p3), and it was run against human 3′UTR or 5′UTR databases [6]. This pattern comprises classical as well as ferritin type IREs with G–U pairing allowed in stems. Proteins with known IREs in their mRNA were discarded from the results; for the remaining IREs a secondary structure was proposed. IREs best fitting the consensus sequence were subjected to further analyses. All sequence alignments were done using National Center for Biotechnology Information (NCBI) BLAST at www.ncbi.nlm.nih.gov/BLAST; sequences used in this study were obtained from NCBI GenBank, and when necessary they were verified by sequencing.

Electrophoretic mobility-shift assay. The human erythroleukemic cell line K562 and the rat intestinal IEC-6 cell line were cultured in RPMI-1640 and DMEM supplemented with insulin, respectively, with 10% fetal calf serum. During the final 24 h, they were treated with 200 μM desferrioxamine (Desf; Desferal, Novartis). Cells were washed twice with ice-cold PBS buffer. The pellet was lysed with ice-cold buffer (40 mM KCl, 25 mM Tris–HCl, pH 7.4, and 1% Triton X-100 [all reagents from Sigma–Aldrich] and protease inhibitor cocktail CompleteMini [Roche]) for 30 min at 4 °C and centrifuged. Supernatant was collected and immediately frozen in liquid nitrogen. Protein concentration was determined by a Bio-Rad protein assay (Bio-Rad).

IRE A from transferrin receptor 1 (TfR) was used as a positive control. DNA templates for T3 RNA polymerase were generated by PCR using T3-TfR and T3-MRCKα primers (Fig. 1A). PCR products were purified by the Wizard SV Gel and PCR Clean-Up System (Promega) and used for RNA preparation. Radioactive probe using [α-^{32}P]ATP as well as a competitor RNA were synthesized in parallel by T3 RNA polymerase (Fermentas) according to the manufacturer's manual. The sequences of expected RNA probes are shown in Fig. 1B. Electrophoretic mobility-shift assay (EMSA) was performed as previously described [7]. Where used, a competitor RNA (0.5, 1, or 2 multiples of the probe concentration) was added to protein lysates (100 μg) for 10 min before the addition of a radioactive probe. Where indicated, 2% (v/v) 2-mercaptoethanol (2ME; Sigma–Aldrich) was added to extracts 5 min before the addition of the probe. Cellular extracts with probe were incubated for 30 min at room temperature; 3 mg/ml heparin was then added for an additional 10 min. RNA/protein complexes were analyzed by 6% non-denaturing polyacrylamide gel electrophoresis, bands visualized by a PhosphorImager FLA2000 (Fuji). Control reactions with TfR IRE probe/TfR IRE competitor and MRCKα IRE probe/MRCKα IRE competitor were run in parallel. All experiments were done several times; representative results are shown.

Change in MRCKα and TfR mRNA expression in response to iron level. Cells of the human hepatocellular carcinoma cell line HepG2 were cultured in DMEM supplemented with 2% fetal calf serum. During the final 24 h they were treated with either 5 μM diferric transferrin (Tf) or 200 μM Desf. Cells grown in quadruplicates were lysed by the direct addition of RNA-Bee (TEL-TEST) and pooled before RNA isolation. RNA isolation was done according to the manufacturer's manual; cDNA was produced using oligo(dT(18)) and SuperScriptII reverse transcriptase (Invitrogen) following the enclosed protocol. The level of *MRCKα* and *TfR* mRNA was measured four times using SYBRGreen (Roche) and RotorGene 3000 equipment (Corbett Research). Expression of glyceraldehyde-3-phosphate dehydrogenase (*GAPDH*) was used as an internal standard. PCR primers

Fig. 1. (A) Sequences of primers (5′ to 3′direction) used in this study. T3 promoter and restriction sites in primers are in bold. F, forward; R, reverse. (B) Expected sequences of RNAs used in EMSA. Predicted IRE hairpin is in bold; nucleotides originating from T3 promoter are in italic.

for *MRCKα*, *TfR*, and *GAPDH* are shown in Fig. 1A. PCR conditions were as follows: initial denaturation (94 °C/5 min) was followed by 40 cycles of denaturation (94 °C/15 s), primer annealing (55 °C/15 s) and elongation (72 °C/45 s). Student's *t* test was used for statistical evaluation.

FACS analysis of the MRCKα IRE activity. To assess the MRCKα IRE activity in vivo, we adopted a system similar to that in references [8,9]. All five TfR IREs with flanking regions (61 bp upstream of IRE A and 75 bp downstream of IRE E) were PCR cloned (primers in Fig. 1A) into the pd2EGFP-N1 plasmid (BD Biosciences Clontech) behind the destabilized variant of the wild type *GFP* with a half-life of ≈2 h. *Not*I and *Xba*I restriction sites were used for cloning. The MRCKα IRE with flanking regions (121 bp upstream and 199 bp downstream of the IRE) was first PCR cloned (primers in Fig. 1A) into the pCR2.1 plasmid using a TA Cloning Kit (Invitrogen). The MRCKα IRE was then excised by *Eco*52I and recloned into the *Not*I site in the pd2EGFP-N1 plasmid. Sequences of all resulting plasmids were verified by direct sequencing.

The human K562 cell line grown in RPMI-1640 with 10% fetal calf serum was transfected with either TfR IREs-, MRCKα IRE-containing vectors or with an empty vector using FuGENE 6 Transfection Reagent (Roche), and stable clones were selected by G418 (1 mg/ml; Sigma–Aldrich). Prior to FACS experiments, the cells were placed in RPMI-1640 supplemented with 2% fetal calf serum and during the final 36 hours were treated with either 5 μM Tf or 200 μM Desf. GFP and DAPI fluorescence was measured by BD FACSAria (BD Biosciences). DAPI staining was used to evaluate the cell viability that was overall >85%. Student's *t* test was used for a statistical evaluation.

Measurement of MRCKα and TfR mRNA stability. Cells of the human hepatocellular carcinoma cell line HepG2 were grown in quadruplicate in DMEM supplemented with 2% fetal calf serum. Where indicated, Desf (200 μM) or Tf (50 μg/ml) was added for 24 h prior to the addition of an inhibitor of transcription. 5,6-dichlorobenzimidazole riboside (DRB, final

concentration 30 μg/ml; Sigma–Aldrich) was added to the culture medium for either 0.5, 1, or 2 h to inhibit transcription. Cells were then lysed by the direct addition of RA1 buffer (Macherey–Nagel) and pooled before RNA isolation. RNA isolation was done using NucleoSpin system (Macherey–Nagel) according to the manufacturer's manual; cDNA was produced using oligo(dT(18)) and SuperScriptII reverse transcriptase (Invitrogen) following the enclosed protocol. The level of *MRCKα* and *TfR* mRNA was measured four times in real time using the same conditions as described above. *GAPDH* was used as an internal standard because its mRNA is stable under various iron concentrations [10].

Tissue specific expression. Relative *MRCKα* and *TfR* mRNA expression was measured in various tissues contained in Human MTC Panel I and Panel II (BD Biosciences). Real-time quantification was done three times using the same conditions as described above.

Results

Identification of putative IREs in 3′UTR of human mRNAs

Using the PatSearch program, we obtained 22 human sequences of a putative IRE lying in 5′UTR and 69 putative IREs lying in 3′UTR. The human UTR database currently comprises more than 150,000 entries, either redundant or non-redundant. Proteins known to carry an IRE in their mRNA were discarded from the set. In the next step, a secondary structure was proposed for all IREs, and the resulting hairpins were evaluated. Criteria for the evaluation were based on the secondary structures of known canonical IRE hairpins: (a) in the upper stem only one G–U pairing allowed within the three middle base pairs; (b) a lower stem at least five base pairs long with less than three G–U. All IREs fulfilling these criteria were further analyzed to answer the following questions: (a) can they be found in EST databases or are they genomic sequences? (b) is the protein known or was it predicted in silico? (c) can orthologs be found in other model organisms? Based on these prerequisites we identified no IRE in 5′UTR and only two putative IREs in 3′UTR—cell cycle phosphatase *Ccd14A* variant 1 (GenBank Accession No. AF000367) and KIAA0451 (GenBank Accession No. AB007920) (Fig. 2A).

The whole CDC14A IRE is 33 nucleotides long with one mismatch in the middle of the lower stem. *CDC14A* variant 1 has only recently been presented to have an IRE in its 3′UTR [11]. *CDC14A* is known to have three transcription variants, but only the variant 1 has IRE in its 3′UTR (Entrez Gene ID: 8556). We therefore focused on *KIAA0451*, which turned out to be identical with *myotonic dystrophy kinase-related Cdc42-binding kinase α* (*MRCKα*; official symbol *CDC42BPA*). The MRCKα IRE starts 784 nt downstream of the stop codon (for comparison, TfR IREs start 882 nt downstream); the remaining part of its 3′UTR from the IRE to the polyA signal is 3600 nt long (in TfR 1200 nt long) (Fig. 2B). The loop contains adenine at the fourth position, and closely resembles TfR IRE A. The stem base pairs are nearly identical with TfR IRE C including the G–U pair in the middle of the stem—of eight base pairs, only one is changed (A–U instead of G–C at the fifth position). The lower stem is A–U rich, which is typical for TfR IREs, with one

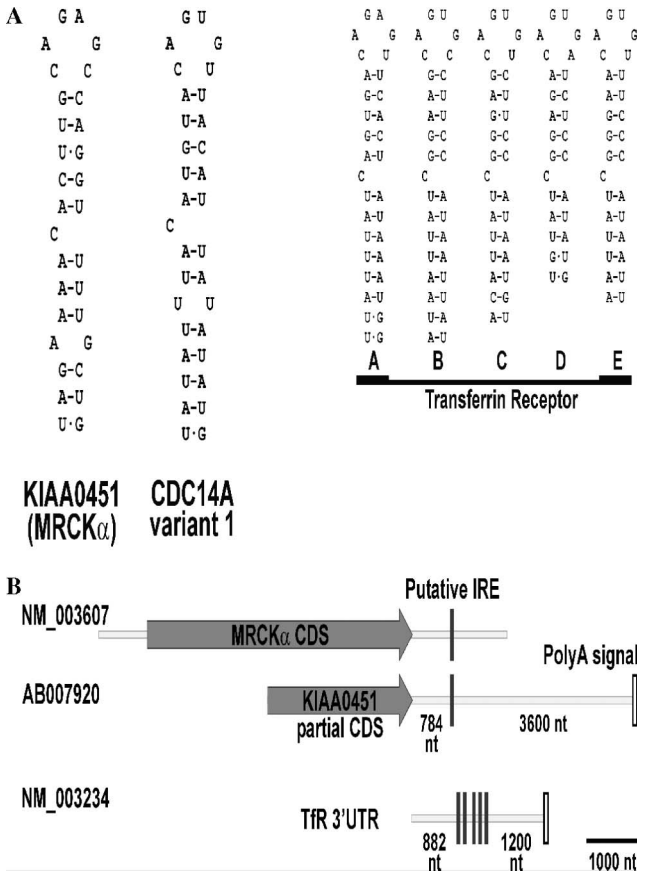

Fig. 2. Identification of putative IREs in human mRNAs. (A) The sequences and secondary structures of human KIAA0451 (MRCKα) and Cdc14A variant 1 IREs are shown. In both cases, the IRE is located in 3′UTR of their mRNA. For comparison, all TfR IRE hairpins are also shown. (B) A putative IRE was identified in 3′UTR of human *KIAA0451* mRNA (GenBank Accession No. AB007920). Nucleotide sequence alignment revealed nearly 100% identity with human *MRCKα* (official symbol *CDC42BPA*). Reference mRNA for human *MRCKα* is shown (GenBank Accession No. NM_003607. For comparison, the structure of *TfR* 3′UTR is also depicted.

mismatch in the middle. The whole hairpin is 31 nucleotides long. Further biochemical analyses were done only with the MRCKα IRE. MRCKα orthologs can be found in a number of organisms, but the IRE hairpin is unique to humans.

IRPs bind the MRCKα IRE in electrophoretic mobility-shift assay

To demonstrate the specificity of the MRCKα IRE/IRPs interaction, three modifications of EMSA were performed. TfR or ferritin IRE is usually used as the competitor in a competitor assay to demonstrate the specificity of IRP binding to the analyzed IRE. In our experiments we used the TfR IRE A hairpin as a competitor in concentrations 0.5, 1, and 2 multiples of the probe concentration. When added to the EMSA prior to the addition of the MRCKα IRE probe, the gradual displacement of the MRCKα IRE from IRE/IRPs complexes can be seen (Fig. 3A).

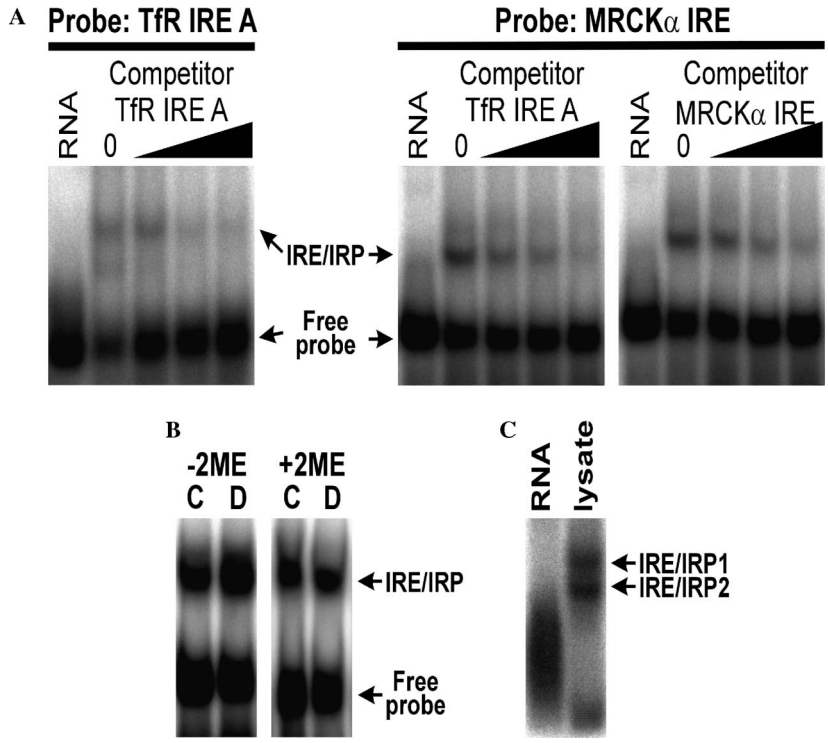

Fig. 3. IRPs bind MRCKα IRE in electrophoretic mobility-shift assay (EMSA). (A) Human TfR IRE A was used as a competitor in EMSA reaction to show the binding of IRPs to the MRCKα IRE. Increasing amount of the competitor (0.5; 1 and 2 multiples of the probe; black triangle above the gels) was added to K562 cell lysates prior to the addition of the radioactively labeled probe. Samples were run on 6% polyacrylamide gel electrophoresis, and gels were scanned by PhosphorImager FLA2000. TfR IRE A used as the competitor can gradually displace the MRCKα IRE from IRP/MRCKα IRE complexes in the concentration-dependent manner. Control reactions with TfR IRE probe/TfR IRE competitor and MRCKα IRE probe/MRCKα IRE competitor were run in parallel. (B) The addition of 2ME increases the activity of IRPs. Control K562 cells [C] exhibited lower, though relatively high, IRPs-binding capacity in comparison with cells treated with iron chelator Desf [D]. The addition of 2ME, however, further increased IRPs activity, resulting in the same values in both groups. The MRCKα IRE was used as a probe. (C) Lysates from rat cells are often used to discriminate between IRP1/IRE and IRP2/IRE complexes. If the MRCKα IRE probe is used with lysates from the rat IEC-6 cell line in EMSA, a typical pattern is observed with two bands likely corresponding to the IRP1/IRE and IRP2/IRE complexes [12].

2ME is used to activate IRPs-binding activity towards IREs. In our conditions, control K562 cells exhibited lower, though relatively high, IRPs-binding capacity in comparison with cells treated with iron chelator desferrioxamine (Desf). The addition of 2ME, however, further increased IRPs activity, resulting in the same values in both groups (Fig. 3B).

Next, we were interested whether the human MRCKα IRE can be also recognized by IRPs from other species, especially whether it can be recognized by both IRP1 and IRP2. For that purpose, we used lysates from rat intestinal IEC-6 cells for two reasons—in rodents two bands can be identified in EMSA, corresponding to the IRE/IRP1 and IRE/IRP2 complexes [12]; and the highest IRP2-binding activity was detected in rat intestine [12]. As shown in Fig. 3C, two distinct bands can be identified, corresponding likely to the IRE/IRP1 and IRE/IRP2 complexes, when lysates from rat intestinal IEC-6 cells were used.

The human MRCKα IRE mediates the response to iron

In the next step, we tested whether the human MRCKα IRE can mediate the response to iron level. Two types of experiments were carried out. To manipulate intracellular iron level, cells of the hepatocellular carcinoma cell line HepG2 were treated with either diferric transferrin (Tf) or iron chelator desferrioxamine (Desf), and the level of *MRCKα* and *TfR* mRNA was measured by real-time quantitative PCR. The level of *MRCKα* mRNA decreased after the Tf treatment (by 8.2%), while after the Desf treatment it increased significantly by nearly 60%, as would be expected for the IRE located in 3′UTR (Fig. 4). Under the same conditions, *TfR* mRNA followed the same behavior, however, with greater dynamics—the level of *TfR* mRNA dropped significantly after the Tf treatment by 60%, while it increased significantly by nearly 700% after the Desf treatment.

To assess the function of the human MRCKα IRE in vivo, MRCKα IRE as well as TfR IREs with flanking regions were cloned behind the destabilized version of the wild type GFP. Transfected K562 cells were selected by G418, and the fluorescence was measured after the addition of Tf or Desf (Fig. 5). After the Tf treatment, the fluorescence of cells carrying the pd2EGFP-MRCKα IRE construct decreased, though not significantly. On the other hand, the addition of Desf led to a significant increase in

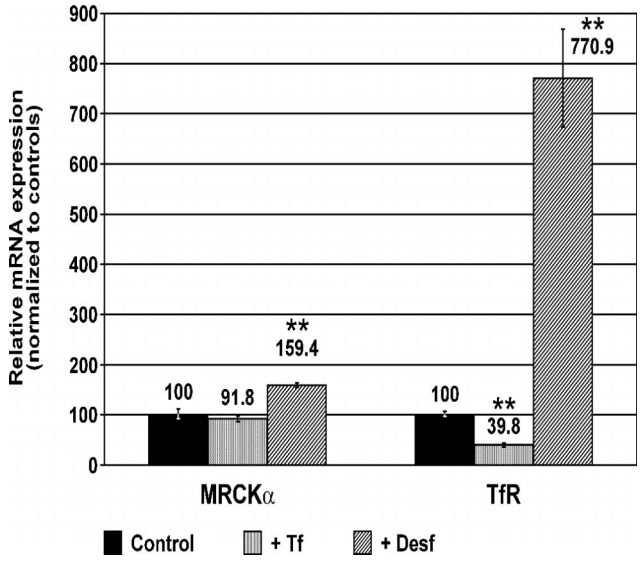

Fig. 4. Changes in the expression of human *MRCKα* and *TfR* mRNA in response to iron. Cells of the human hepatocellular carcinoma cell line HepG2 were treated with either 5 μM Tf or 200 μM Desf for 24 h. After the addition of Tf, the level of mRNA dropped by 8.2% and 60.2% in *MRCKα* and *TfR*, respectively. When Desf was added, an increase in mRNA level by 59.4% and 670.9% was noted for *MRCKα* and *TfR*, respectively. Means and standard deviations of four experiments are indicated. Expression was normalized to non-treated controls. Student's *t* test was used for statistical evaluation. $^{**}p < 0.005$.

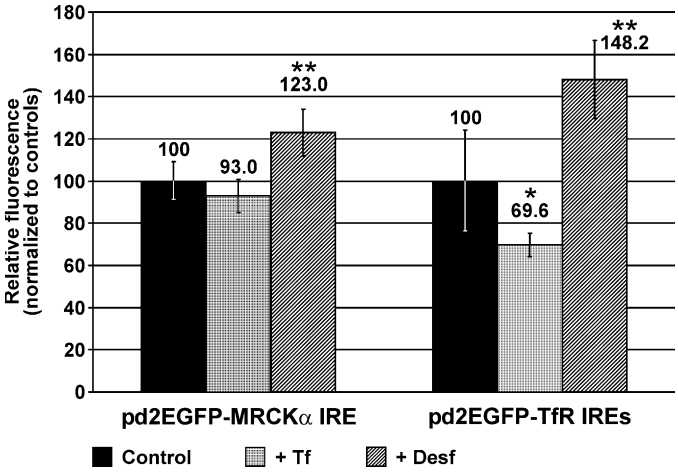

Fig. 5. FACS analysis of the K562 cell line transduced with the pd2EGFP plasmid carrying either MRCKα IRE or TfR IREs A to E cloned behind GFP. In the Tf-rich medium (5 μM) the fluorescence decreased by 7% and 30.4% in pd2EGFP-MRCKα IRE and -TfR IREs, respectively. After the addition of Desf (200 μM), the fluorescence increased by 23% and 48.2% in pd2EGFP-MRCKα IRE and -TfR IREs, respectively. Fluorescence was normalized to non-treated controls. Means and standard deviations of five experiments are indicated. Student's *t* test was used for statistical evaluation. $^{*}p < 0.05$; $^{**}p < 0.005$.

mean cellular fluorescence by 23%. Cells with *EGFP* controlled by all five TfR IREs acted in the same manner, although again with greater dynamics (decrease by 30% after the Tf treatment; increase by 48% after the Desf addition). Results from both types of experiments therefore indicate that the human MRCKα IRE mediates the response to iron level in the same way as TfR IREs.

The human MRCKα mRNA stability is controlled by iron levels

To be flexibly posttranscriptionally regulated by IRPs, mRNA must be short-lived. We therefore measured the half-life of the human *MRCKα* mRNA in the HepG2 cell line. DRB was added to the cell culture for up to 2 h to stop transcription, and kinetics of *MRCKα* and *TfR* mRNA decay was studied (Fig. 6). If Desf was added to the culture medium, both *MRCKα* and *TfR* mRNA became stable with a half-life >2 h. On the other hand, after the Tf treatment, both *MRCKα* and *TfR* mRNA were more rapidly degraded (half-lives 45 and 30 min, respectively) in comparison with untreated controls (half-lives 70 and 90 min, respectively). We also used another inhibitor of transcription, actinomycin D, but unfortunately it interferes with an iron-dependent degradation of *TfR* mRNA [13] as well as *MRCKα* mRNA (our unpublished observation). However, in Desf- and Tf-untreated controls we obtained results similar to those from DRB experiments (the half-lives 75 min and nearly 2 h for the *MRCKα* and *TfR* mRNA, respectively; data not shown). The level of the control gene *GAPDH* did not change in response to a treatment. We conclude that *MRCKα* mRNA is short-lived, and its stability is regulated by iron levels.

Expression of the human MRCKα mRNA correlates with TfR expression in various tissues

Finally, we tested the level of *MRCKα* and *TfR* mRNA expression in various tissues. *MRCKα* is differentially expressed in all tissues tested, with the highest levels found in testes, and the lowest in skeletal muscle (Fig. 7). Surprisingly, the level of mRNA expression of human *MRCKα* strongly positively correlates with the *TfR* expression (15 tissues, Spearman's rank correlation coefficient 0.8393; $p = 0.0017$ at the 95% confidence level), indicating that MRCKα might be somehow involved in the Tf iron uptake pathway.

Discussion

In this study, we used a biocomputational approach in combination with biochemical methods to identify novel IREs in human mRNAs. Out of more than 73,000 entries in the non-redundant and 76,000 entries in the redundant human UTR databases, only two new IREs fulfilled the criteria we set for a consensus IRE—cell cycle phosphatase *Cdc14A* variant 1 and *KIAA0451* (Fig. 2A). Interestingly, cell cycle phosphatase *Cdc14A* variant 1 has recently been presented to possess an IRE in its 3′UTR [11], confirming the feasibility of our approach. With respect to the number of entries in UTR databases that very likely cover the whole human transcriptome (it is

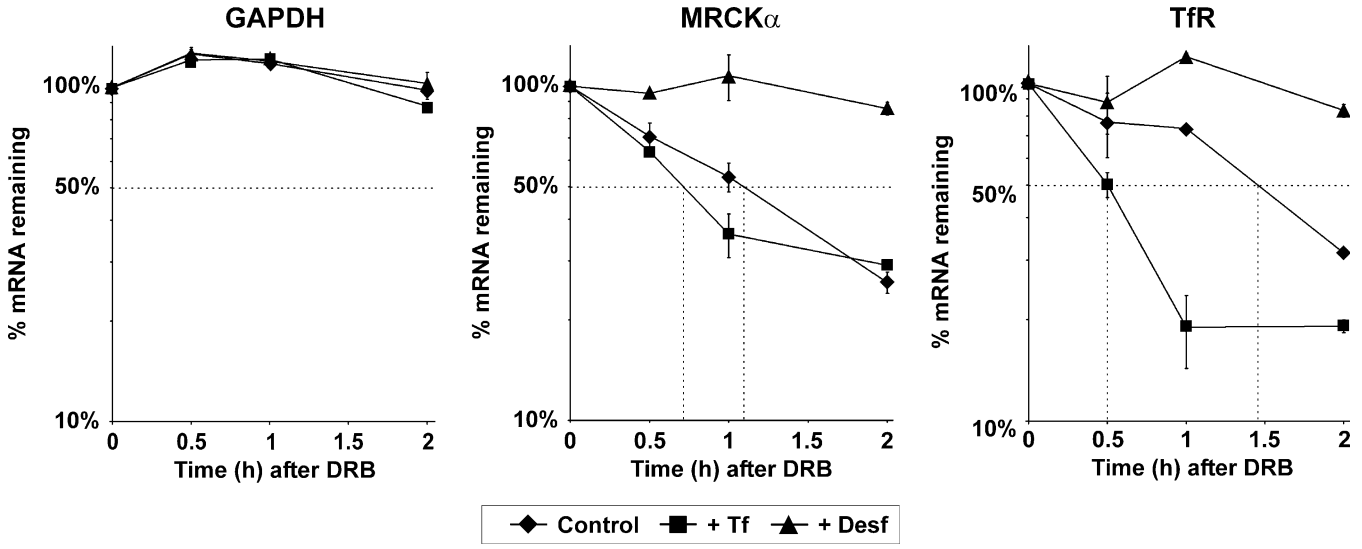

Fig. 6. Stability of *MRCKα* and *TfR* mRNA. HepG2 cells were grown in a medium supplemented with either transferrin (Tf; 50 μg/ml) or desferrioxamine (Desf; 200 μM) for 24 h. For times indicated, the inhibitor of transcription DRB (30 μg/ml) was added to a culture medium, and the stability of *MRCKα* and *TfR* mRNA was measured. Both *MRCKα* and *TfR* mRNA became stable after the Desf treatment, while they are more rapidly degraded after the Tf treatment in comparison with untreated controls. *GAPDH* was used as a control gene. Means and standard deviations of four experiments are shown.

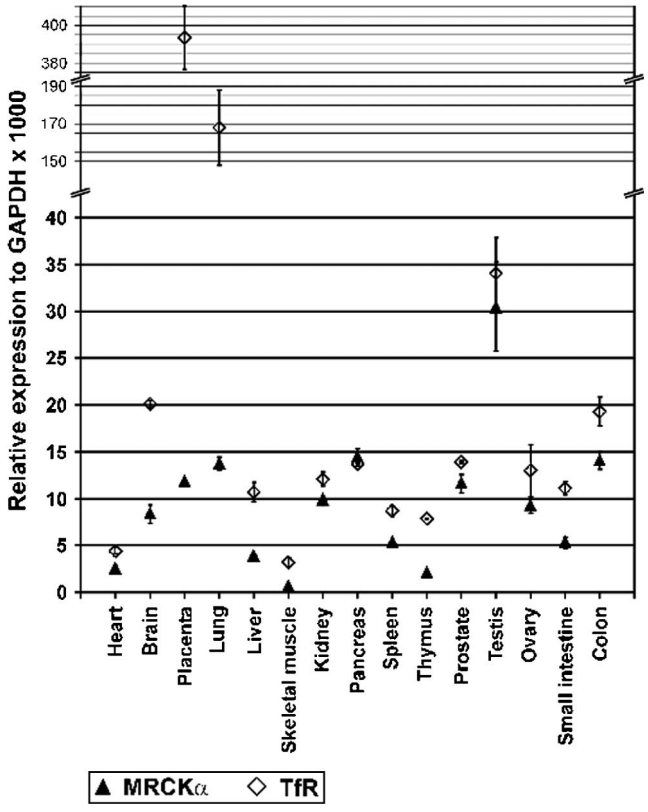

Fig. 7. The relative expression of *MRCKα* and *TfR* mRNA in various tissues. The highest expression of *MRCKα* mRNA among tissues tested was observed in testes; the lowest expression was noted in skeletal muscle. Three measurements were done; means and standard deviations are indicated. Spearman rank correlation test was used to evaluate the relationship between the level of *MRCKα* and *Tfr* mRNA expression in various tissues. Spearman rank correlation coefficient was 0.8393, indicating that a highly significant positive correlation exists between *MRCKα* and *Tfr* mRNA expression (15 tissues, $p = 0.0017$ at the 95% confidence level).

estimated that human genome contains 20,000–25,000 genes encoding proteins [14]), we believe that we have possibly identified all canonical IREs in humans. The command used for the PatSearch program, however, does not cover non-canonical IREs (e.g., IRE in one isoform of *DMT1*), and thus some functional IREs can still be awaiting identification.

In further analyses, we focused on *KIAA0451* that was identical with *MRCKα*. The MRCKα IRE loop sequence CAGAGC has already been studied during the investigation of the optimal sequence and structure of IRE. In both studies (clone 21 in the reference [15]; clone 155 in the reference [16]), the loop sequence CAGAGC exhibited nearly the same or even higher-binding affinity towards both IRP1 and IRP2 proteins in comparison with the wild type sequence CAGUGC. Binding to both IRPs was also confirmed by our EMSA results. When lysates from the rat intestinal IEC-6 cell line were used in the EMSA reaction, two similarly intensive bands likely corresponding to IRP1/IRE and IRP2/IRE complexes [12] can be observed (Fig. 3C). As for the stem structure, its base pairing is nearly the same as in the TfR IRE C (7 base pairs out of 8 are identical; Fig. 2A). It was shown that the TfR IRE C alone had the ability to function as the translational IRE [17]. In summary, the MRCKα IRE should be in theory one of the "strongest" IRE elements, and our results support this assumption.

We employed several techniques to show that the MRCKα IRE binds to IRPs, and it functions in response to iron level in the same manner as TfR IREs do, though with lower dynamics. Under conditions of low iron, the MRCKα IRE mediated the significant increase in mRNA and protein level (Figs. 4 and 5), while after the Tf treatment a decrease in mRNA and protein levels, though

non-significant, was observed. The lower response of the MRCKα IRE could be attributed to three facts – (1) *MRCKα* mRNA contains only one IRE compared to *TfR* with five IREs (Fig. 2B); (2) the TfR expression is also regulated at the transcriptional level by hypoxia inducible factor (HIF-1) under conditions of low iron [18]; (3) cells in the Tf-rich medium rapidly internalize surface transferrin receptors and degrade *TfR* mRNA, saving the cells from an acute iron overload. Indeed, the addition of Tf to a culture medium resulted in a rapid degradation of *TfR* mRNA (the half-life decreased 3–4 times from 1.5–2 h to 30 min), while the half-life of *MRCKα* mRNA decreased less than 2 times from 70–75 min to 45 min (Fig. 6). On the other hand, under conditions of iron deprivation both *MRCKα* and *TfR* mRNA are stabilized with a half-life >2 h. These findings were probably also reflected in the observation that both the MRCKα IRE and TfR IREs responded with greater dynamics to iron chelator desferrioxamine, in contrast to lower dynamics when Tf (i.e., receptor-mediated uptake) was used as a source of iron. Taken together, our results indicate that *MRCKα* mRNA is unstable, and its stability is controlled by intracellular iron levels via the IRE in its 3′UTR.

However, how is *MRCKα* mRNA degradation regulated? It was demonstrated that the *TfR* mRNA degradation involved an endonucleolytic cleavage and did not involve poly(A) tail shortening [19,20]. The cleavage site was localized directly behind the IRE C, but the recognition site is not found in *MRCKα* mRNA. We therefore searched the *MRCKα* 3′UTR for AU-rich elements AUUUA (AREs) that are typically located in the 3′UTR of short-lived mRNAs such as protooncogenes and cytokines [21]. AREs act as regulators of mRNA stability, because they can usually promote its degradation by activating both decapping and deadenylation processes. The human *MRCKα* 3′UTR contains eight AREs, three are clustered within 200 nt upstream of the IRE; the rest is dispersed throughout the 3′UTR. The last ARE is located 100 nt from the polyA site, being perfectly complementary to miR16. miR16 is a human microRNA containing a UAAAUAUU sequence that is complementary to the ARE sequence, and it seems to be essential in ARE-mediated mRNA degradation [22]. Further experiments should therefore address relationships between miR16/AREs-RNA decay and IRE/IRPs stabilization of *MRCKα* mRNA.

MRCKα protein is well conserved among various species, but the IRE hairpin is unique to humans. It is not for the first time for a functional IRE to be identified in only one species. For instance, a functional IRE was identified in 5′UTR of *Drosophila melanogaster succinate dehydrogenase b* [23,24], or in 3′UTR of mouse *glycolate oxidase* [25]. Interestingly, when the human MRCKα IRE with flanking regions (cca. 340 bp) is compared with the chimpanzee genome (build 1), only two mismatches can be found, and both are located in the chimp IRE-like sequence (one in the loop, the second in the upper stem), likely disrupting the hairpin folding. It is therefore tempting to speculate that the functional MRCKα IRE in humans represents an evolutionary advantage. While chimpanzees remained during evolution mostly plant eating (>87–98% of their annual diet is taken from plant sources), it is believed that the routine inclusion of meat and animal source foods in the diet was mandatory for emergence of the human lineage [26]. *MRCKα* may thus be one of "meat-adaptive" genes that were selected to confer resistance to disease risks associated with meat eating [27].

MRCKα is a serine/threonine kinase that acts as a downstream effector of Cdc42, which is a member of the Rho subfamily of small GTPases (together with Rho and Rac) [28], which are known to regulate the cytoskeleton. MRCKα and Cdc42 were shown to be involved in neurite outgrowth [29], in filopodia formation [28,30], and together with Rho-ROCK signaling they cooperate in cell invasion [31]. It has been published recently that Cdc42-MRCKα also regulates nuclear movement in polarizing cells in a myosin II-dependent manner [32]. As for the underlying molecular mechanisms, MRCKα can regulate myosin assembly by phosphorylation of the myosin-binding subunit (MBS, MYPT1) of myosin-light chain phosphatase [31] and myosin regulatory-light chain II, at least in vitro [5]. It can also phosphorylate LIMK1 and LIMK2 kinases that regulate actin assembly [33]. MRCKα therefore seems to regulate the cytoskeleton in response to signals transmitted by Cdc42 by influencing actin/myosin filament assembly and activity [34].

Why should be *MRCKα* mRNA regulated by iron levels? It is of interest to note that Cdc42 was found taking part in endocytosis, but the direct cooperation with MRCKα during this process has not yet been studied [35,36]. Recently, endosome involvement in iron targeting to mitochondria was documented in erythroid cells [37]. More importantly, the authors have demonstrated that both the myosin light-chain kinase inhibitors, wortmanin and the calmodulin antagonist W-7, caused significant inhibition of iron incorporation from iron-loaded Tf endosomes into heme, suggesting that myosin is required for Tf-vesicle movement. Since Cdc42 was localized within a transferrin receptor-positive endosomal compartment (at least in breast carcinoma cells) [38], these findings open up the possibility of a direct involvement of MRCKα in this process.

Interestingly, the highest expression of MRCKα was found in testes. Indeed, iron is essential for male fertility, and disruption of iron balance leads to impairment of testicular function (e.g., in hemochromatosis; OMIM: 235200). It has been known for some time that spermatocytes carry TfR on their surface, and as a source of iron they exclusively utilize Tf, which is produced by Sertoli cells [39]. Moreover, DMT1 was immunolocalized to both Sertoli and germ cells, and was suggested to play a role in transporting iron between intracellular compartments as it does in other tissues [40]. It is therefore tempting to speculate that MRCKα could regulate Tf-vesicle movement through actin/myosin filament assembly in response to iron

level, and in cooperation with other IRE-regulated proteins (TfR, ferritin, and DMT1), they could precisely tune iron uptake from Tf. This hypothesis is also supported by our finding that the level of *MRCKα* mRNA in various tissues strongly positively correlates with the level of *TfR* mRNA (15 tissues, Spearman's rank correlation coefficient 0.8393; $p = 0.0017$ at the 95% confidence level; Fig. 7), further emphasizing the intriguing possibility of MRCKα involvement in the Tf iron uptake pathway.

Taken all together, our results indicate that human MRCKα should be added to the list of proteins, whose mRNA stability is regulated by intracellular iron levels via the IRE sequence present in their 3′UTR. Additional studies should then unveil the precise role of MRCKα in cellular machinery and its link to iron metabolism.

Acknowledgments

The work was supported by Grant 204/04/P150 from the Grant Agency of the Czech Republic. We thank David Hardekopf and Daniel Vyoral for a critical reading of the manuscript, and Tomas Kalina and Pavel Semerak for technical help with FACS analyses.

References

[1] R.S. Eisenstein, K.P. Blemings, Iron regulatory proteins, iron responsive elements, and iron homeostasis, J. Nutr. 128 (1998) 2295–2298.
[2] K. Pantopoulos, Iron metabolism and the IRE/IRP regulatory system: an update, Ann. N. Y. Acad. Sci. 1012 (2004) 1–13.
[3] E.C. Theil, R.S. Eisenstein, Combinatorial mRNA regulation: iron regulatory proteins and iso-iron-responsive elements (Iso-IREs), J. Biol. Chem. 275 (2000) 40659–40662.
[4] M.W. Hentze, M.U. Muckenthaler, N.C. Andrews, Balancing acts: molecular control of mammalian iron metabolism, Cell 117 (2004) 285–297.
[5] T. Leung, X.Q. Chen, I. Tan, E. Manser, L. Lim, Myotonic dystrophy kinase-related Cdc42-binding kinase acts as a Cdc42 effector in promoting cytoskeletal reorganization, Mol. Cell. Biol. 18 (1998) 130–140.
[6] F. Mignone, G. Grillo, F. Licciulli, M. Iacono, S. Liuni, P.J. Kersey, J. Duarte, C. Saccone, G. Pesole, UTRdb and UTRsite: a collection of sequences and regulatory motifs of the untranslated regions of eukaryotic mRNAs, Nucleic Acids Res. 33 (2005) D141–D146.
[7] V. Picard, F. Renaudie, C. Porcher, M.W. Hentze, B. Grandchamp, C. Beaumont, Overexpression of the ferritin H subunit in cultured erythroid cells changes the intracellular iron distribution, Blood 87 (1996) 2057–2064.
[8] J.Y. Li, G. Ram, K. Gast, X. Chen, K. Barasch, K. Mori, K. Schmidt-Ott, J. Wang, H.C. Kuo, C. Savage-Dunn, M.D. Garrick, J. Barasch, Detection of intracellular iron by its regulatory effect, Am. J. Physiol. Cell Physiol. 287 (2004) C1547–C1559.
[9] R.J. Henderson, S.M. Patton, J.R. Connor, Development of a fluorescent reporter to assess iron regulatory protein activity in living cells, Biochim. Biophys. Acta 1743 (2005) 162–168.
[10] H. Gunshin, C.R. Allerson, M. Polycarpou-Schwarz, A. Rofts, J.T. Rogers, F. Kishi, M.W. Hentze, T.A. Rouault, N.C. Andrews, M.A. Hediger, Iron-dependent regulation of the divalent metal ion transporter, FEBS Lett. 509 (2001) 309–316.
[11] M. Sanchez, G. Bruno, M.W. Hentze, M.U. Muckenthaler, A novel IRE in the cell cycle phosphatase CDC14A, 1st Congress of the International Bioiron Society (2005) 45.
[12] B.R. Henderson, C. Seiser, L.C. Kuhn, Characterization of a second RNA-binding protein in rodents with specificity for iron-responsive elements, J. Biol. Chem. 268 (1993) 27327–27334.
[13] C. Seiser, M. Posch, N. Thompson, L.C. Kuhn, Effect of transcription inhibitors on the iron-dependent degradation of transferrin receptor mRNA, J. Biol. Chem. 270 (1995) 29400–29406.
[14] International Human Genome Sequencing Consortium, Finishing the euchromatic sequence of the human genome, Nature 431 (2004) 931–945.
[15] B.R. Henderson, E. Menotti, C. Bonnard, L.C. Kuhn, Optimal sequence and structure of iron-responsive elements. Selection of RNA stem–loops with high affinity for iron regulatory factor, J. Biol. Chem. 269 (1994) 17481–17489.
[16] B.R. Henderson, E. Menotti, L.C. Kuhn, Iron regulatory proteins 1 and 2 bind distinct sets of RNA target sequences, J. Biol. Chem. 271 (1996) 4900–4908.
[17] J.L. Casey, M.W. Hentze, D.M. Koeller, S.W. Caughman, T.A. Rouault, R.D. Klausner, J.B. Harford, Iron-responsive elements: regulatory RNA sequences that control mRNA levels and translation, Science 240 (1988) 924–928.
[18] L. Bianchi, L. Tacchini, G. Cairo, HIF-1-mediated activation of transferrin receptor gene transcription by iron chelation, Nucleic Acids Res. 27 (1999) 4223–4227.
[19] R. Binder, J.A. Horowitz, J.P. Basilion, D.M. Koeller, R.D. Klausner, J.B. Harford, Evidence that the pathway of transferrin receptor mRNA degradation involves an endonucleolytic cleavage within the 3′ UTR and does not involve poly(A) tail shortening, EMBO J. 13 (1994) 1969–1980.
[20] M.W. Hentze, L.C. Kuhn, Molecular control of vertebrate iron metabolism: mRNA-based regulatory circuits operated by iron, nitric oxide, and oxidative stress, Proc. Natl. Acad. Sci. USA 93 (1996) 8175–8182.
[21] A. Bevilacqua, M.C. Ceriani, S. Capaccioli, A. Nicolin, Post-transcriptional regulation of gene expression by degradation of messenger RNAs, J. Cell. Physiol. 195 (2003) 356–372.
[22] Q. Jing, S. Huang, S. Guth, T. Zarubin, A. Motoyama, J. Chen, F. Di Padova, S.C. Lin, H. Gram, J. Han, Involvement of microRNA in AU-rich element-mediated mRNA instability, Cell 120 (2005) 623–634.
[23] N.K. Gray, K. Pantopoulos, T. Dandekar, B.A. Ackrell, M.W. Hentze, Translational regulation of mammalian and *Drosophila* citric acid cycle enzymes via iron-responsive elements, Proc. Natl. Acad. Sci. USA 93 (1996) 4925–4930.
[24] S.A. Kohler, B.R. Henderson, L.C. Kuhn, Succinate dehydrogenase b mRNA of *Drosophila melanogaster* has a functional iron-responsive element in its 5′-untranslated region, J. Biol. Chem. 270 (1995) 30781–30786.
[25] S.A. Kohler, E. Menotti, L.C. Kuhn, Molecular cloning of mouse glycolate oxidase. High evolutionary conservation and presence of an iron-responsive element-like sequence in the mRNA, J. Biol. Chem. 274 (1999) 2401–2407.
[26] K. Milton, The critical role played by animal source foods in human (Homo) evolution, J. Nutr. 133 (2003) 3886–S3892.
[27] C.E. Finch, C.B. Stanford, Meat-adaptive genes and the evolution of slower aging in humans, Q. Rev. Biol. 79 (2004) 3–50.
[28] A. Hall, Rho GTPases and the actin cytoskeleton, Science 279 (1998) 509–514.
[29] X.Q. Chen, I. Tan, T. Leung, L. Lim, The myotonic dystrophy kinase-related Cdc42-binding kinase is involved in the regulation of neurite outgrowth in PC12 cells, J. Biol. Chem. 274 (1999) 19901–19905.
[30] N. Nakamura, N. Oshiro, Y. Fukata, M. Amano, M. Fukata, S. Kuroda, Y. Matsuura, T. Leung, L. Lim, K. Kaibuchi, Phosphorylation of ERM proteins at filopodia induced by Cdc42, Genes Cells 5 (2000) 571–581.
[31] S. Wilkinson, H.F. Paterson, C.J. Marshall, Cdc42-MRCK and Rho-ROCK signalling cooperate in myosin phosphorylation and cell invasion, Nat. Cell Biol. 7 (2005) 255–261.

[32] E.R. Gomes, S. Jani, G.G. Gundersen, Nuclear movement regulated by Cdc42, MRCK, myosin, and actin flow establishes MTOC polarization in migrating cells, Cell 121 (2005) 451–463.
[33] T. Sumi, K. Matsumoto, A. Shibuya, T. Nakamura, Activation of LIM kinases by myotonic dystrophy kinase-related Cdc42-binding kinase alpha, J. Biol. Chem. 276 (2001) 23092–23096.
[34] Z.S. Zhao, E. Manser, PAK and other Rho-associated kinases—effectors with surprisingly diverse mechanisms of regulation, Biochem. J. 386 (2005) 201–214.
[35] N.K. Hussain, S. Jenna, M. Glogauer, C.C. Quinn, S. Wasiak, M. Guipponi, S.E. Antonarakis, B.K. Kay, T.P. Stossel, N. Lamarche-Vane, P.S. McPherson, Endocytic protein intersectin-l regulates actin assembly via Cdc42 and N-WASP, Nat. Cell Biol. 3 (2001) 927–932.
[36] W.S. Garrett, L.M. Chen, R. Kroschewski, M. Ebersold, S. Turley, S. Trombetta, J.E. Galan, I. Mellman, Developmental control of endocytosis in dendritic cells by Cdc42, Cell 102 (2000) 325–334.
[37] A.S. Zhang, A.D. Sheftel, P. Ponka, Intracellular kinetics of iron in reticulocytes: evidence for endosome involvement in iron targeting to mitochondria, Blood 105 (2005) 368–375.
[38] M. Parsons, J. Monypenny, S.M. Ameer-Beg, T.H. Millard, L.M. Machesky, M. Peter, M.D. Keppler, G. Schiavo, R. Watson, J. Chernoff, D. Zicha, B. Vojnovic, T. Ng, Spatially distinct binding of Cdc42 to PAK1 and N-WASP in breast carcinoma cells, Mol. Cell. Biol. 25 (2005) 1680–1695.
[39] B.G. Vannelli, C. Orlando, T. Barni, A. Natali, M. Serio, G.C. Balboni, Immunostaining of transferrin and transferrin receptor in human seminiferous tubules, Fertil. Steril. 45 (1986) 536–541.
[40] K.P. Griffin, D.T. Ward, W. Liu, G. Stewart, I.D. Morris, C.P. Smith, Differential expression of divalent metal transporter DMT1 (Slc11a2) in the spermatogenic epithelium of the developing and adult rat testis, Am. J. Physiol Cell Physiol. 288 (2005) C176–C184.